Composites Part A 128 (2020) 105643

Contents lists available at ScienceDirect

Composites Part A

journal homepage: www.elsevier.com/locate/compositesa

Mitigating forming defects by local modification of dry preforms

Mark A. Turk[a,*], Bruno Vermes[b], Adam J. Thompson[a], Jonathan P.-H. Belnoue[a], Stephen R. Hallett[a], Dmitry S. Ivanov[a,*]

[a] Bristol Composites Institute (ACCIS), Advanced Composites Collaboration for Innovation and Science, University of Bristol, University Walk, Bristol BS8 1TR, UK
[b] Department of Polymer Engineering, Budapest University of Technology and Economics, H-1111 Budapest, Muegyetem rkp. 3, Hungary

ARTICLE INFO

Keywords:
A. Preform
B. Defects
C. Numerical analysis
E. Forming

ABSTRACT

Forming of dry fibre textile pre-forms is a commonly used technique to achieve complex shapes for light weight composite structures. Most conventional engineering fabrics can only deform through shearing. Excessive shearing often results in the formation of detrimental features, such as wrinkles, folds and fabric distortions. This paper shows the feasibility of improving formability by local modification of preforms in critical areas to enhance forming and mitigate against defects. Modification is implemented by printing localised resin patches onto textile preforms. The technique allows for continuity of fibres throughout the preform with the additional benefit that the deposited resin can be thermally staged to the desired level of cure to tune the viscosity of the region for forming and consolidation. The location and dimensions of patches are specified through numerical modelling to inform the subsequent manufacturing process. Manufacturing trials successfully demonstrate the possibility of defect mitigation using this technique.

1. Introduction

Resin infusion offers great advantages in rate of manufacture and cost reduction over pre-preg based techniques. An integral step prior to the infusion and curing process is the forming of the reinforcement material into the final part geometry, this process is prone to various defects associated with the intrinsic properties of textile preforms: low out-of plane buckling resistance, minimal extensibility in the fibre directions, low initial shear stiffness and exponential stiffening at high angles of shear. Inextensibility of preforms in the fibre direction results in difficulties of forming the fabric to a complex shape without generating distortions or out-of- plane buckling of reinforcement, known as wrinkling.

Optimisation of the forming procedure to minimise the occurrence of defects is a well explored area in composites manufacturing, which has led to a number of established methods. Broadly speaking, available techniques fall into two categories: constraining the fabric at the perimeter of the forming domain, or locally modifying the fabric at critical locations within the preform area. Methods of fabric constraint at the perimeter include the use of blank holders [1–4], tensioning elements [5,6], or flexible tracking devices [7]. Fabric constraint allows for the elimination of areas with compressive in-plane stresses. Such compression can occur when parallel fibres in an originally flat preform are formed onto a complex tool. Fibre lengths on a formed shape may be different for each of the individual fibre paths. When the difference in neighbouring paths is significant, preform shearing takes place, but it may not always be sufficient to accommodate the length difference without causing compression. Blank holders and tensioning elements compensate for the negative stresses and allow the achievement of higher shear angles without wrinkling. Pre-tensioning of the fabric is effective but requires a complex system of fabric constraints and may be limited in the shapes it can efficiently handle.

Localised preform modification relies on a different mechanism. If the area where a defect is likely to occur is known, then modifying preform properties in this area can change the deformation map and drive the defect away from the critical location. Modification of the preform properties can increase buckling stiffness and prevent excessive shearing. Such gradient distribution of properties, if arranged carefully, can delocalise shearing deformations and prevent defect formation. This preform modification has been demonstrated through stitching [8], tufting [9], activation of yarns commingled with thermoplastic fibres [10], variation of weave patterns [11], and tensioning elements [6]. Local through-thickness stitching of a single - or multi-ply preform hinders the relative movement of the warp and weft fibres at the crossover points and therefore influences the shear behaviour and the formability of the fabric. The location, direction, pattern and density of

* Corresponding authors.
E-mail addresses: mark.turk@bristol.ac.uk (M.A. Turk), dmitry.ivanov@bristol.ac.uk (D.S. Ivanov).
URL: http://www.bristol.ac.uk/composites/ (M.A. Turk).

https://doi.org/10.1016/j.compositesa.2019.105643
Received 1 July 2019; Received in revised form 5 September 2019; Accepted 21 September 2019
Available online 23 September 2019
1359-835X/

the seams are all important parameters and for advanced preform formability their optimisation is necessary. It has been shown that in some cases stitches outside the shear zones have a more significant effect on drapability than those inside these zones [8]. Stitching also improves the through-thickness mechanical properties of the final composite and influences the in-plane properties in a way that depends on a number of factors (e.g., material, stitching method, loading scenario, etc.) [12]. Likewise, tufting of multi-ply preforms was shown to have a potential to significantly reduce the wrinkling of preforms [9]. A very different approach is implemented using Jacquard weaving machines which are capable of creating fabrics with locally modified weave architectures [11]. Combining fabric weaves with different architectures in the same preform sheet leads to gradient formability characteristics. This helps to provide good stability at non-complex, mechanically critical areas and good formability at shear zones.

Localised modification of the preform is especially valuable in scenarios where creating constraints at the perimeter is either overly complex, too time consuming, or too costly, leading to disproportionate challenges for implementation and automation. Local modification on the other hand has the potential to negatively impact the internal cohesion of the structure and hence damage the mechanical properties of the finished part. There is also the potential for tufting or stitching to distort fibres leading to a reduction of the in-plane strength of the component.

In this study an alternative preform modification technique is proposed. It builds on the work of Vermes et al. [13,14] which investigated the potential for changing preform properties through the introduction of resin patches. The approach is similar in scope to Liquid Resin Print [15,16] and, as opposed to other approaches, has a minimal impact on the internal architecture of the reinforcements. Thermosetting fast curing resin is deposited locally into regions where high shearing is expected and then thermally staged to the desired level of cure to tune the viscosity of the region for forming and consolidation. Viscous deposited resin changes the interaction between fibres. Patched regions remain deformable but exhibit a notably stiffer response compared to surrounding dry material. This affects the shear angle distribution across the component.

Multiple process parameters of local patching need to be established to make it effective. One set of parameters relate to the geometrical position of the patches. Shape, orientation, size, location and distribution of patches all make a clear impact on the possibility of mitigating defects. An incorrect patch pattern may actually negatively affect the shear angle distribution and defect likelihood. Another set of parameters relate to the properties of the patches. Deposition of reactive resin gives the potential to take advantage of a wide range of viscosities that can be achieved through thermal treatment and hence, tune bending/shear resistance of the fabric. As will be shown in this paper, the patch properties do influence shear map distribution. On the other hand, the additional material parameters result in greater optimisation space but increase the complexity of optimisation. This complexity makes numerical simulations an essential part of this process.

The development of modelling capabilities to help understand and predict defect formation has been the focus of a substantial research effort. Overviews of modelling techniques for forming can be found in [17] and [18]. Homogenised constitutive equations for biaxial fabric are formulated as hypo-elastic [18] or hyper-elastic models [19,20] and implemented in a finite-element framework for a continuous sheet of shell elements. Modelling attempts have been largely successful in capturing the in-plane rotations of the fibre directions, predictions of wrinkle sites and, more recently, the shape and size of wrinkles in single layer forming processes [3,21,22]. The development of such models has identified the necessity to capture the shear behaviour of the textile preform in models correctly, as it has proven to be the fundamental mechanism behind fibre re-orientation [3,23,24], whereas out-of-plane bending stiffness is essential to make accurate predictions of the shape and size of wrinkles [3,21]. More recent modelling efforts have concentrated on including more complex deformation mechanisms into constitutive models, these include in-plane bending stiffness [25], through thickness deformation [26] and the dissipative behaviour of textiles which is required to capture the effects of unloading [27].

There exists a wealth of numerical modelling techniques that can be used for forming optimisation. Optimisation strategy can be complex when forming with a mould as the forming scenario can be highly sensitive to initial parameters. Due to the complex and highly non-linear nature of fabric behaviour during mould closure it is difficult to identify the ideal initial setup. The process therefore lends itself to optimisation through iteration with a wide variety of initial patch configurations trialled in a systematic basis. Vermes et al. [14], using a discrete model inspired by Skordos et al. [28], performed a systematic parametric search aimed at minimisation of the shear angle. This paper builds on the initial work reported in [13] and adapts a similar pragmatic two-step optimization strategy: at first the position of large bulk patches is selected from a short list of several likely optimum positions, then a detailed forming is considered to refine the exact geometry of patch position in the selected domain. In contrast with previous results, the optimization is performed using a 2D element approach suggested by Thompson et al. [29,30] and similar to [31]. It combines shell and membrane element formulations to present a realistic balance of bending and in-plane tensile properties of the preform. This study looks at both the conventional measure of critical deformation – shear angle [4,5,11,13,14,18] and a direct observation of wrinkling provided by the model. The latter is used as an independent measure of success of patch optimisation placement. The findings from the numerical study are then used to inform physical forming experiments to establish the effectiveness of patch placement for mitigating defects.

2. Component geometry

The test case, chosen for this study, is a non-structural component with exaggerated geometry. Kinematic drape simulations suggest that this component is not formable [13] – independently of drape starting point and initial fabric orientation the shear angle in some locations approaches 90°. This does not however mean that the component cannot be formed in principle – it means that it is not possible to align fabric reinforcement with the geodesic lines and hence, an additional material treatment is needed. The challenge set by this study is to explore the feasibility of making such a component formable by applying stabilising elements through liquid injected resin.

The component is thin-walled and doubly symmetric as shown in Fig. 1. It is tapered towards the centre with characteristic dimensions of approximately 230 mm in length and 30–50 mm in width. The maximum height at location A-A′ is approximately 25 mm. This geometry is chosen as it is sufficiently complex to present forming difficulties without being excessively difficult or impossible to form. The geometrical features include convex and concave corners, tapers, ramps and other double curvature features. It is envisaged that a wide range of geometries could be readily assessed using the approach to patch placement shown below.

The process considered for the manufacture of this component is liquid resin infusion of a dry biaxal preform. The essential driver for the choice of processing technique is to minimize manual intervention such as sequential draping operations. Hence, the infusion must be preceded by deep drawing forming and consolidation of the fabric. This paper focuses on describing the forming process and defect mitigation for an isolated layer of material only. It is important to emphasize that defects associated with the forming of a multi-layer stack can be of a different nature (e.g., due to inter-ply/inter-tool friction [32–34], consolidation factors [35], and non-biaxial symmetry of the preform) and need to be addressed separately.

Kinematic simulations of this geometry with fabric aligned with the component symmetry axes show excessive shearing at the regions of B-B′ to C′-C and along the concave corner P′Q′D′ (see Fig. 1) – well above

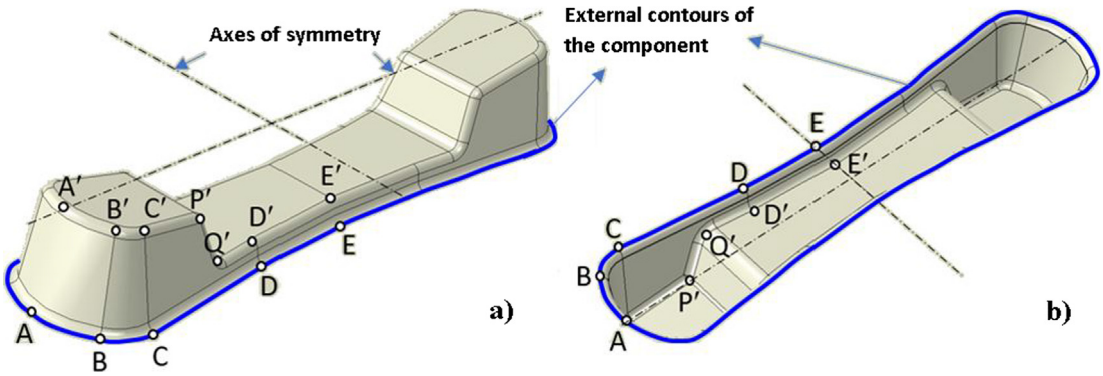

Fig. 1. Geometry of the (a) male and (b) female moulds of the component. (For interpretation of the references to colour in this figure legend, the reader is referred to the web version of this article.)

the locking angle (when the lateral interaction of sheared yarns causes out of plane buckling of fabric). As shown later, full forming simulations predict similar issues. Hence, the process requires interference in redistribution of the shear angle to mitigate the occurrence of critical defects.

3. Numerical tool for patch placement.

3.1. Model formulation/description

In order to identify the best locations for stiffened zones, numerical simulations were conducted. For this a continuous 2D surface representation of the fabric was adopted. Following the approach suggested by Khan et al. [22] it uses a hypo-elastic model implemented into a VUMAT user material subroutine for Abaqus explicit. The model defines shear stress-strain response in the coordinate system associated with the orientation of warp/weft yarns and tracks the fibre reorientation to ensure correct stress computation for material undergoing large deformations. An important further development suggested by Thompson et al. [29,30], includes the superposition of shell and membrane elements to realistically represent both the high in-plane tensile stiffness and low out of plane bending stiffness, an important characteristic of fibrous and woven materials. Thus, the model correctly captures the dominant features of fabric behaviour: fibre rotation, shear stiffening, uncoupled bending and tension responses. In addition, the continuous formulation makes it more computationally efficient and numerically stable than the discrete model tried previously [13]. All these features make it an appropriate and rational choice for the purposes of patch placement optimisation.

Driven primarily by the needs of patch position design, the shear stiffness of both the patched and non-patched region is considered to be non-linear and increasing exponentially with shear angle, with the unpatched fabric having a lower initial stiffness and higher locking angle. The shear behaviour is described by the polynomial expression in Eq. (1) which gives the shear stiffness, G_{12}, as a function of the inter-fibre shear angle, γ [30].

$$G_{12}(\gamma) = 193.8\gamma^5 - 253.3\gamma^4 + 121.9\gamma^3 - 21.53\gamma^2 + 0.9932\gamma + 0.05827 \quad (1)$$

The slight non-monotonic variations in shear stiffness at low shear angles is a widely observed behaviour introduced by the boundary conditions of the picture frame shear test and can be seen in a number of studies [36,37]. Compared to the large shear deformations observed in forming over the studied shape these variations are negligible and do not affect the solution. At present, there is no established methodology for patch property identification. In the presented simulation the focus is on contrast between the properties of the patches and the fabric, whereas the exact properties of the preform are less important. Hence, the generic properties of a characteristic fabric have been used as the input for the material model [30]. The fundamental features of the solution, such as the defect location/orientation and trends in shear angle distribution, are likely to be preserved when exact properties are tuned. Overall, numerical trials with variation of these properties and experimental trials presented in Section 4 confirm this assumption. Due to the model parameters not being matched to the specific fabric considered in the manufacturing trials later, the purpose here is to inform patch placement and not to simulate exact forming behaviour.

In a first set of simulations, the shear stiffness of resin patch regions were artificially increased by 10 MPa whereas the shear stiffness in the bulk material defaults to a near negligible value, both patched and bulk material subsequently increase non-linearly with shear angle. The bending resistance of the patch regions was kept the same as that of the bulk material, which is justified by the off-axis orientation of the patch as discussed further in Section 4.3. Other properties were chosen to be approximately representative of woven fabric. For the membrane elements (M3D4R) a Young's modulus of 35,000 MPa was assigned to the fibre directions whereas the shell elements (S4R) were assigned a modulus of 50 MPa equivalent to a bending rigidity of 0.52 Nmm^2 for an element thickness of 0.5 mm, to represent the low bending stiffness. The shell elements were given five integration points. Both element types were assigned a thickness of 0.5 mm.

The mould included a flat area outside the component contour of 250 × 250 mm in-plane dimensions. The meshed fabric was created to be slightly larger than the mould in-plane (see Fig. 2) and was meshed with quadrilateral elements. It is possible that fabric size will influence the resulting wrinkle pattern, consequently these dimensions were chosen to be similar in size to the experiments of Section 4. The choice of preform dimensions in the experiments on the other hand was chosen by the motivation to minimise the influence of edge effects. A Coulomb friction model with a penalty algorithm was used to model contact between the fabric and the mould. A small coefficient of friction ($1\,0^{-6}$) was added to stabilize the numerical solution. A geometrical pre-processor for the forming simulations was created in Python to assign the position, size (height/width), orientation and the number of rectangular patches parametrically. The mesh size was set at a seed spacing of 2 mm for both the fabric and the mould, with an analysis time of 10 s. Male and female moulds are simulated to be un-deformable rigid body shell elements (S3R, S4R) with the male mould slightly smaller than the female by 1.6 mm allowing space for the fabric once closed, which is characteristic of the actual mould gap used in the experiments of Section 4 and also essential for model convergence. A PC with the following specifications has been used for the simulations: 3.4 GHz, 4 Cores, 8 Logical Processors, 16 GB RAM.

A mesh sensitivity study was carried out to ensure that the model outputs were not overly influenced by mesh size. It was found that mesh sizes with characteristic linear dimensions larger than 3 mm generally caused the run to crash due to excessive distortion of the mesh. On the other hand, mesh sizes lower than 1 mm caused excessive run time. A

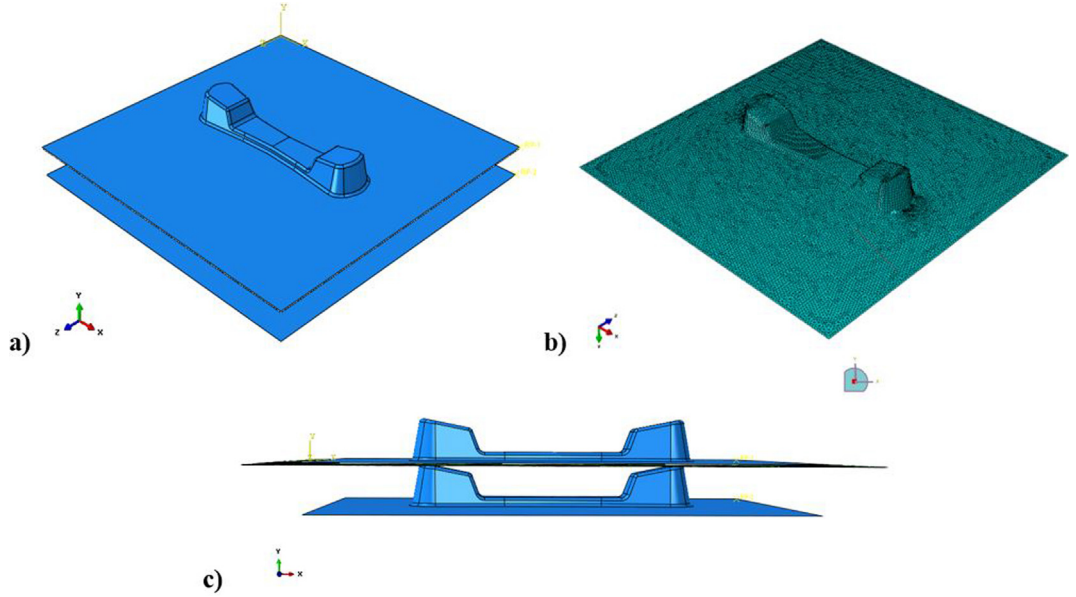

Fig. 2. (a) Matching moulds (b) top view of meshed male mould (c) moulds with fabric shown between. (For interpretation of the references to colour in this figure legend, the reader is referred to the web version of this article.)

significant change in shear angle resulted from the reduction in mesh size from 3 mm to 2 mm, this then levelled out and no further significant change was found in reducing further to 1 mm. It was also found that to reliably achieve full mould closure with a range of patch combinations whilst avoiding premature failure of the run a meshsize of 1 mm was needed, however 2 mm was generally adequate for achieving partial closure (60% or better). The reason for this premature failure was due to the mesh size being too coarse prohibiting the mesh from closely following the contours of the component, which combined with the assumption of incompressibility in the through thickness direction blocks full closure. On this basis the 2 mm mesh size was chosen as a good balance of accuracy and achievable run time. A few exceptions to this were made, and these are noted where they occur later in the paper.

3.2. Forming of non-stabilised material

The finite element model described above was first applied to explore forming of non-stabilised material over the tool geometry. The results of these simulations are shown in Fig. 3. In this case the mesh size was maintained at 2 mm on the basis that this is refined enough to capture the onset of wrinkles and still be indicative of where patches should ideally be placed. As shown later reducing the mesh size to 1 mm results in successful full closure of the mould with the associated cost in run time (15 h rather than 3 h, with 4CPU).

Even at incomplete closure the wrinkle pattern is revealed well. It can be seen that one large fold occurs in the preform at each corner in the region BC with the fold tip propagating towards B'C'. The position of this wrinkle is consistent with the locations of highest shear angle. The primary challenge of patch placement is therefore to eliminate the major wrinkles or to drive them away from the contours of the component shape. Due to the fact that the position of the wrinkles in this instance correlates with high shearing it seems intuitively correct to start with changing the shear response in those regions.

3.3. Optimisation strategy

Optimisation of patch position and patch properties can be a difficult task. The parametric space is vast, while every simulation is computationally demanding. Traditional optimisation procedures cannot therefore be applied here, particularly when the purpose of the simulations is a process design rather than sophisticated analysis of all the aspects of forming. In this paper, a pragmatic optimisation strategy is taken. While this approach is not universal it can be easily adapted to other geometries. The process optimisation is divided onto two steps. At the first stage, called 'rough optimisation', we explore an approximate

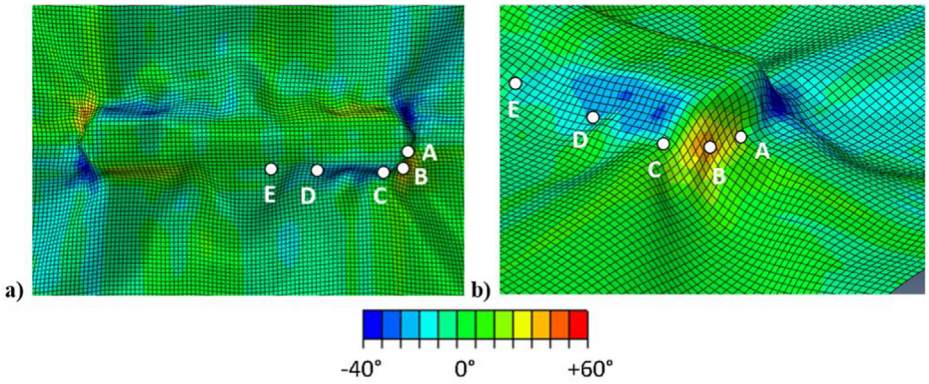

Fig. 3. Shear angle distribution in forming simulation without stabilising patches (female mould hidden). (a) top view, (b) side view on critical region B-B′-C′-C. (For interpretation of the references to colour in this figure legend, the reader is referred to the web version of this article.)

location of patches out of a limited number of possible candidates, defined based on specific features of geometry. The purpose of the first step is to narrow down the optimisation space. The patches considered in the first step cover relatively large areas compared to feature sizes. The results of the simulations at this stage are indicative only.

The optimisation criteria, in agreement with conventionally used criteria [4,5,11,13,14,18], is maximum shear angle. Whilst not necessarily the best criterion for indication of wrinkle occurrence, at this stage it provides a good understanding of the intensity of shear deformations. This is based on the assumption that once the fabric exceeds its locking angle, out of plane deformation is unavoidable. This is an effective method for assessing formability at a first approximation, but it has limitations. A high shear angle does not guarantee the presence of a wrinkle. In fact, wrinkles often manifest a situation when more favourable out-of-plane loss of stability occurs at lower shear angles or at zero shear. It does however give some ideas about whether localised modifications can work for redistributing potential problems to outside of the area of concern. An alternative approach to wrinkle identification based on buckling behaviour rather than shear angle has been assessed by Matveev et al. [38].

For the purpose of computational efficiency the simulations are not run to completion but stopped at sufficient closure depth (approximately 60%). Hence, at this level of closure a likely wrinkle may not yet necessarily have formed. The output of these simulation are used then to assess critical areas where the patches need to be positioned. At the second stage; a) patch geometry is refined: instead of bulk patches narrower zones are used, which as discussed further appear to be more suitable, and b) precise patch position in the targeted region is defined in several targeted simulations. The success of the patch positioning at the second stage is evaluated by direct examination of wrinkle intensity predicted by the forming simulations rather than by shear magnitude.

3.4. Rough forming optimisation using bulk patching

Placing bulk patches is based on understanding of critical locations where shear deformations may be high and shear bands narrow. Increased material resistance in selected regions is expected to delocalize fabric deformation, redistribute the shear angle over a larger area, minimise the magnitude of shearing in the regions of interest, and hence reduce the probability of defect occurrence. Especially in instances when geometry is complex and contains multiple critical regions, choosing the positioning of the stabilising elements correctly is difficult. Stabilising material in one location may lead to a defect in a different location.

In the initial design stage, four major zones were selected as candidates for stabilisation, the dashed lines in Fig. 4 mark the perimeter of the patches. Zones 1 and 3 were the areas of potentially highest shear concentration in concave and convex corners, whereas zones 2 and 4 bridge them. This gave 16 possible combinations ranging from no zones stabilised (reference case) to all zones stabilised. At this stage, the most successful combination was deemed to be the one where maximum

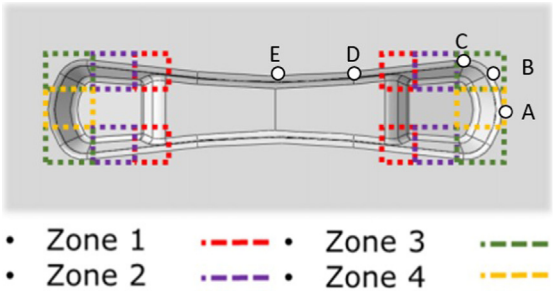

Fig. 4. Definition of zones for introducing stabilising elements. (For interpretation of the references to colour in this figure legend, the reader is referred to the web version of this article.)

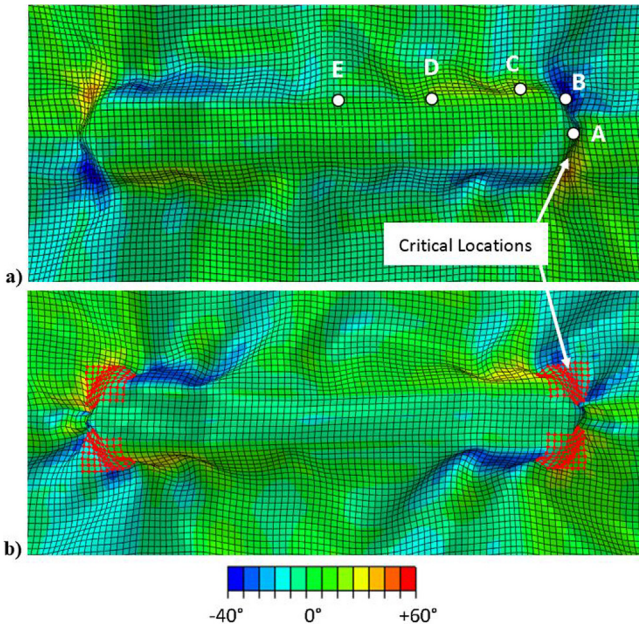

Fig. 5. Comparison of shear maps in (a) reference (non-stabilised) and (b) stabilised configurations (zone 3) at 60% closure. (For interpretation of the references to colour in this figure legend, the reader is referred to the web version of this article.)

shear angle within the shape of the component is minimal. The patch dimensions were set at 16 mm × 20 mm with an initial shear stiffness of 10 MPa. Not all the simulations out of 16 could be brought to successful completion and some of the simulations were aborted before the moulds were in full contact. Hence, for fair comparison, all the forming simulations were stopped at 15 mm upper mould displacement out of 25 mm required for complete closure, at this deformation the results for all the runs could be successfully derived

The simulations showed that bulk patching generally results in a noticeably worse outcome than the unpatched reference run, with a few exceptions where the configuration was of comparable effectiveness. The most promising patch configuration at 60% closure, with the exception of the reference case, was to place stiffer material in zone 3 (see Fig. 5). Stabilisation slightly increased the maximum intensity of the shear from 42° to 43°. This also led to a shift in the location of maximum shearing. However, as well as slightly increasing the overall shear angle the rough stabilisation introduced more areas of instability with larger folds appearing. Instead of localized wrinkles, one or more large folds tend to appear – Fig. 6. Variation of the bending rigidity of the patched regions for the zone 3 configuration in the range of 0.01 N mm^2–100 N mm^2 resulted in fluctuation of maximum shear in the 40–50° window. The worst configuration was found to be stabilising zones 1, 2, 3 and 4 resulting in a maximum shear angle at 60% closure of 54°, it is unsurprising that such excessive stiffening of the fabric should give the worst result. It is apparent at this stage that bulk patching is not producing a better result than the unstiffened configuration, however it does provide useful information to inform patch placement.

Bringing the mould to full closure required a mesh size of approximately 1 mm rather than 2 mm to avoid premature termination of the run, which becomes prohibitive when attempting to run 16 different combinations. However, once the optimal patch configuration was established, this configuration was successfully brought to full closure with a mesh size of 1 mm giving a final maximum shear angle of 65° with zone 3 stiffened. Full closure for the unstiffened configuration gave the slightly higher maximum shear angle of 67° by contrast. A comparison of the shear maps of these two runs is shown in Fig. 6.

Comparing Figs. 5 to 6 the contrast in fabric behaviour can be

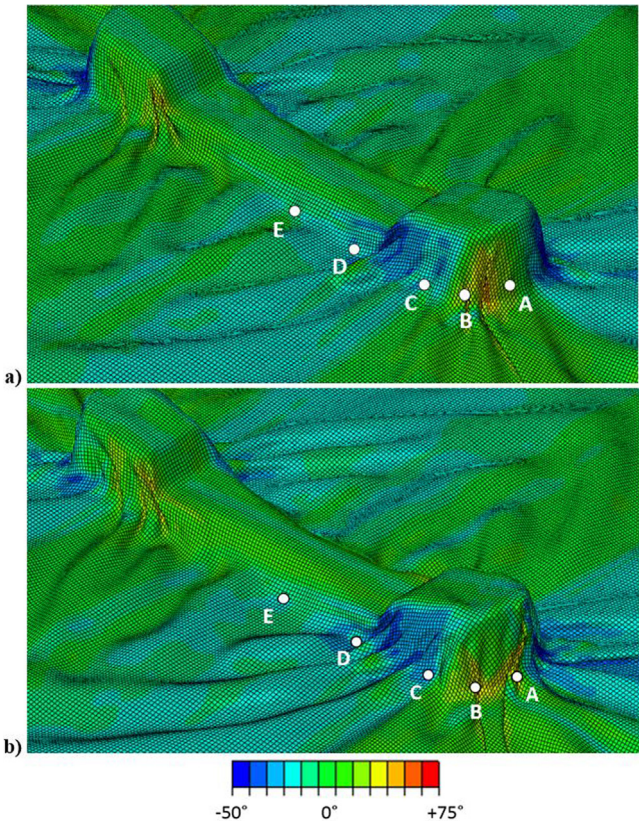

Fig. 6. Comparison of shear maps in (a) reference (non-stabilised) and (b) bulk stabilised configurations (zone 3) at full mould closure. (For interpretation of the references to colour in this figure legend, the reader is referred to the web version of this article.)

clearly seen at 60% closure as well as an indication of the number of winkles or folds. Full closure is nonetheless needed to have clarity on the severity of wrinkles and their final location.

3.5. Line patches placement

The sequence of bulk patching simulations helps to rule out the options where the interference with material properties lead to a worse wrinkling situation. Based on the well-documented trials on the role of bending-stiffness/shear resistance ratio [18], it could be hypothesized that to avoid large folds associated with contrasting properties, it is desirable to maintain resistance to shear but at the same time to avoid ramping up the bending stiffness.

To achieve this, we suggest the addition of diagonal (with respect to yarn direction) line patching in the region of interest rather than bulk patching. Patches introduced at an angle to the fibre direction can help to decouple bending response of the patches from high tensile stiffness of yarns.

The new stabilisation approach where narrow patches of 25 mm in length and 5 mm in width were placed in the regions B-B' and C-C' (see Fig. 1) was trialled and the simulation results are shown in Fig. 7. Note that in this run full mould closure was achieved by using a mesh size of 1 mm.

Fig. 7b shows the line patch locations. The model predicted a maximum shear angle of 70° which is a slight increase compared to 67° for the unstiffened scenario (see Fig. 6a). The model demonstrates the redistribution of wrinkles in the critical location and the formation of two large folds outside the shape of the component (contrasted to one large fold in the unstiffened case). It is key to note that the line patching did not result in the additional cost of substantial instability elsewhere as is observed for the bulk patching (Fig. 6b). This gives an indication

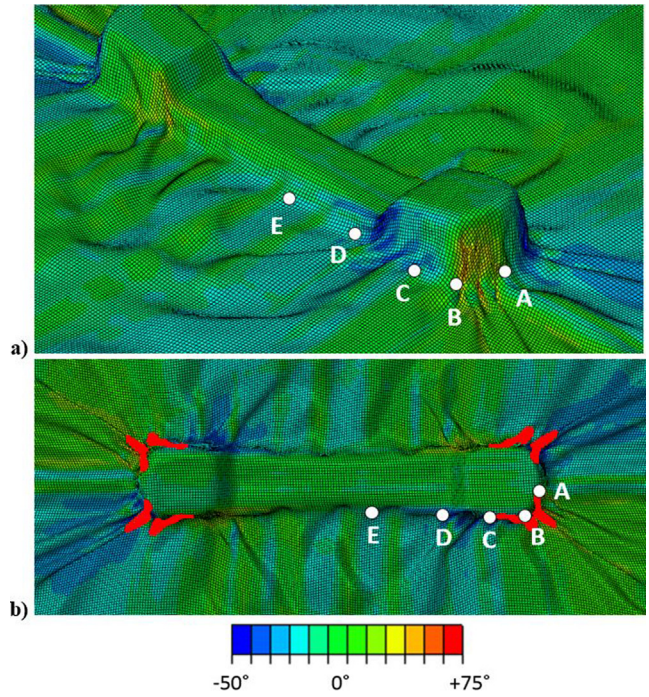

Fig. 7. (a) Shear angle distribution resulting from forming simulations with stabilising line patches (patch locations hidden) (b) top view with patch locations shown in red. (For interpretation of the references to colour in this figure legend, the reader is referred to the web version of this article.)

that by using line patching it is possible to flexibly tailor a fine balance between bending and shear resistance and potentially reduce wrinkling instabilities in the preform.

3.6. The effect of patch properties on wrinkle likelihood

One of the advantages of patching with liquid thermosetting resin is that by thermal treatment, particularly if it is a snap-curing system, a wide range of viscosities and hence, patch properties can be achieved. To better understand the sensitivity of the model to patch properties the initial shear stiffness of the bulk patches was varied for the zone 3 only configuration (see Fig. 4) whilst all other parameters remained the same. As discussed previously, the highest shear angle over the entire domain is chosen as the measure of model sensitivity and the mould is closed only to 60% closure. Results are also compared to the baseline configuration (no patching). Note that the patch behaviour remains non-linear as explained in Section 3.1, the values quoted here are the initial constant values.

Results are plotted in Fig. 8. It can be seen that the model is sensitive to variations in shear stiffness and shear angle can vary by up to 10° over a relatively narrow distribution of shear stiffness. It can also be seen that the trends are non-monotonic and can hardly be intuitively predicted. From this plot the model suggests an optimal initial patch shear stiffness of approximately 50 MPa for this arrangement of patch locations, it is important to bear in mind however that this is not a representative value as the model parameters have not been matched to actual material properties. It can be seen that the effect of the shear stiffness on maximum shear angle is not linear but precise tuning of the patch properties are shown to be important. The shear angle is not measured from the same location in each run, rather it is the highest shear angle appearing anywhere in the modelled fabric. The higher shear angles at higher shear stiffness can be explained as the much stiffer patches lock up regions of the fabric making it harder for the remaining material to conform to the mould geometry, leading to wrinkling. An observation of the contrast between the wrinkle patterns

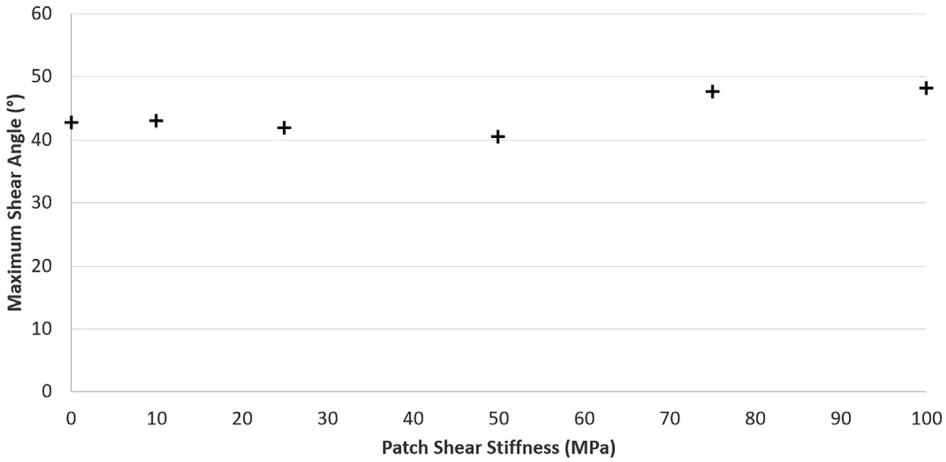

Fig. 8. Variation of maximum shear angle with shear stiffness.

for the best scenario (50 MPa shear stiffness) and the worst scenario (100 MPa shear stiffness) reveals minimal difference in the deformation pattern. Due to the considerably longer runtimes and propensity of the model to abort before completion when using high shear stiffnesses and full mould closure (due to excessive distortion of the elements) we were unable to produce a similar graph to Fig. 8 at full closure.

4. Experimental trials for preform stabilization

Experimental trials were carried out in a direct forming experiment using a single layer of reinforcement constrained between two rigid moulds. The Acrylonitrile Styrene Acrylate moulds of the same geometry as shown in Fig. 2 were manufactured using Fused Deposition Modelling technique with a resolution of 0.1 mm. A 2/2 twill E-glass reinforcement sheet of 280 g/m^2 areal density and a repeating unit length of 5 mm was chosen for trials based on its balance between formability and excessive bundle deformations. Sheets of 350 mm × 200 mm were cut from the fabric in 0°/90° fibre orientation. An ink grid of ~8.5 mm cell-size was stamped onto one side of each sheet, still in its flat undeformed state to track and visualize shear deformation. In some instances, the patch free fabric was uniformly sprayed with epoxy spray binder to maintain the deformed shape after opening of the mould. For the double contact forming, a 6 kg weight was placed on top of the male mould to close the moulds and apply the consolidation pressure. After reaching the gel-point, the male mould was removed to examine the shear pattern of the fabric, the form of which was preserved by the resin and/or the spray binder.

4.1. Resin conditioning

For the preform stabilization, a fast curing epoxy resin system was chosen. The Huntsman Araldite LY3585 epoxy and the Aradur 3475 hardener were mixed in a 100:21 wt ratio. The resin was injected into the fabric at the predefined stabilization zones using fine needles to avoid fibre distortion. In the case of line patching narrow resin bands were placed at 45° to the fibre directions along lines B-B' and C-C' (see Fig. 1). Deposited as narrow bands, these quickly widened due to the capillary forces. Therefore cornflour was mixed into the resin prior to the injections in a 100:60 ratio of mixed resin to powder to increase its viscosity, thereby reducing the capillary effect. Thermal tuning of resin viscosity was carried out by conditioning of the injected resin using a heated flat press. At the first stage, the heated plate is brought into contact with the impregnated fabric without applying pressure. At the second stage the fabric is consolidated and transferred to forming. Duration and temperature of heating has to be chosen to ramp up the degree of cure (DoC), and hence, the resin viscosity, to a controlled level but prior to vitrification. Based on prior resin characterization the gel point was identified at a conversion rate of 40–50%. The forming trials were carried out after taking the resin in stabilized areas to a conversion rate of 10% (70 °C for 2 min) and 30% (70 °C for 4 min).

4.2. Bulk patching forming trials

Based on the suggested patch locations given by the numerical observations, both bulk patching and line patching were implemented in a series of experiments:

A. Reference trial where no liquid resin was applied.
B. Spray binder over the whole surface of the fabric.
C. Three trials where resin patches were brought to DoCs of 0%, 10% and 30% prior to forming.

Problems were anticipated in ensuring that the reference sample retained its deformation once the male mould was removed, hence the second spray binder sample was considered to prevent this spring back effect. After forming, the fabric was left on female mould and examined optically.

Fig. 9 shows the shear map of the formed fabric. In the spray binder case significant wrinkling of the fabric occurred, the injected but untreated fabric and low degree of cure fabric also showed problems with wrinkling. The highest degree of cure resin caused the most significant change in the shear pattern appearing to reduce wrinkle occurrence though instead causing a major fold to appear. The cause of folding was traced back to the increased bending stiffness at the stabilized zones due to the patch-wise applied resin. In agreement with the simulations, the experimental trials showed that a modified stabilization approach was needed that would maintain the local resistance to shearing without causing an excessive rise in bending stiffness.

4.3. Line patching forming trials and model validation

Following indicative numerical simulations, the off-axis line injection patches were considered as an alternative to bulk patching. The work is presented as a series of separate case studies with issues and improvements outlined at each stage.

4.3.1. Line patching case study 1

Initial trials A-C above highlighted two significant problems. Firstly, spray binder was found to be unsuitable as a reference case due to the high shear stiffness this imposed (see Fig. 10). Binder made it both hard to maintain the deformed shape after removal from the mould and very resistant to shearing, it was therefore decided to remove the spray

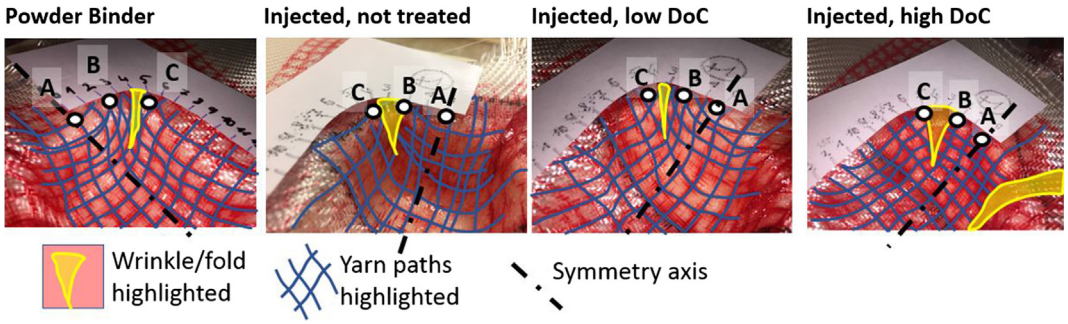

Fig. 9. Shear map of the bulk patch injected fabrics. (For interpretation of the references to colour in this figure legend, the reader is referred to the web version of this article.)

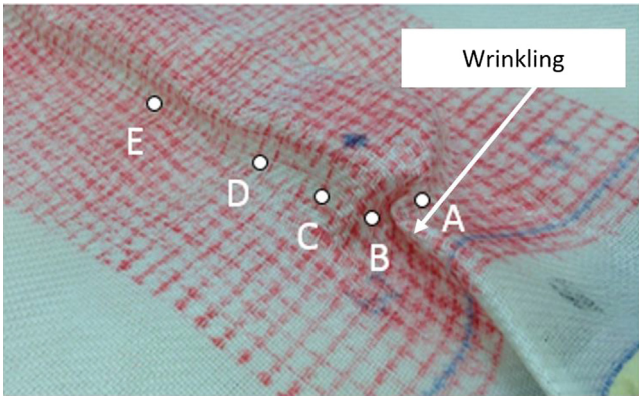

Fig. 10. Spray binder reference sample. (For interpretation of the references to colour in this figure legend, the reader is referred to the web version of this article.)

binder case from the trial.

Secondly, as anticipated, the dry reference sample lost much of its deformation pattern upon removal of the male mould due to spring back and therefore this data is unreliable as a reference case. In order to obtain a full closure deformation pattern for the reference unstiffened case, a sample was created identically to case A, except that the fabric had been soaked briefly in water beforehand. The results of this experiment are shown in Fig. 11 with both moulds now removed.

This modification had the slightly unintended result of significantly increasing friction with the mould, which in effect introduced tensioning to the forming trial. This resulted in a sample with much reduced wrinkling and excellent adherence to the mould once the male mould was removed. However, as the purpose of this experiment was to create a suitable reference case this improved formability was not appropriate for comparison purposes, nor was it suitable for applying across the board due to the risk of these effects outweighing any observable impact of patch placement.

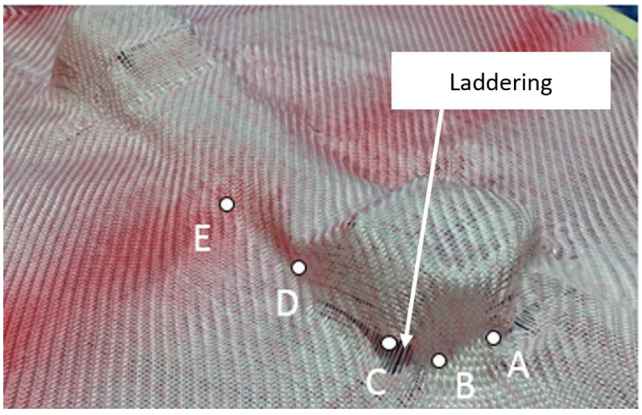

Fig. 11. Wet fabric reference sample (unstiffened). (For interpretation of the references to colour in this figure legend, the reader is referred to the web version of this article.)

Therefore, due to the unsuitability of soaking the whole fabric, a small amount of water was instead applied to the troughs in the female mould before closure. This created two shallow wells, thereby taking advantage of the surface tension and extra weight (once capillary action had wetted the wider area of fabric) to avoid losing the deformation pattern once the male mould was removed. The water was placed in such a way as to only come into contact with the fabric very near to full mould closure so as to avoid any influence on the results. This procedure was also carried out for the samples with resin patches (as well as for the reference sample) for consistency.

With these amendments implemented trials A and C above were carried out and the observed forming results are shown in Fig. 12. Once demoulded the samples were sprayed thoroughly with spray binder to maintain the deformation.

It can be seen that in this trial all samples successfully avoid significant wrinkling with the exception of the high DOC patching case where two wrinkles span the height of the corner either side of one resin patch (highlighted in yellow). In this case there is a shift in the centrality of the fabric leading to the patches being off centre. However, it was also observed in this trial that 'laddering' was occurring (see Fig. 12) where parallel tows are dragged away from each other leading to distortions and openings in the fabric. This was predominantly due to localised friction forces arising during mould closure. This laddering is detrimental for composite performance, and although the previous discussions were mostly focused on wrinkling, this defect needs to be eliminated in manufacturing practice as well. Differences in forming behaviour at different patch stiffnesses is roughly in agreement (i.e., correct description of locations with maximum shear intensity, correct indication of positions of major wrinkles or folds, correct description of the fabric contours) with the numerically observed effects, however full comparison can not be made due to fibre distortions.

The no cure and low degree of cure scenarios are difficult to distinguish between in terms of successfulness, this distinction is further complicated by the various defects shown. The low DoC scenario has therefore been chosen to carry forward into the next case study along with the dry fabric baseline due to ease of handling when compared to no cure and greater contrast in patch properties when compared to dry fabric. Fig. 13 shows the shear map of the low degree of cure formed fabric from Fig. 12 illustrating the shear angles along path A-B-C-D-E for each of the four corners. It can be seen that the shear map varies significantly depending on which corner is examined and the forming result is non symmetrical despite a symmetrical mould. This behaviour was also observed in the simulations. Due to this lack of symmetry it is difficult to quantify a comparison between the simulation results and manufacturing trials based on measured shear angle, instead the equivalent images will be visually compared.

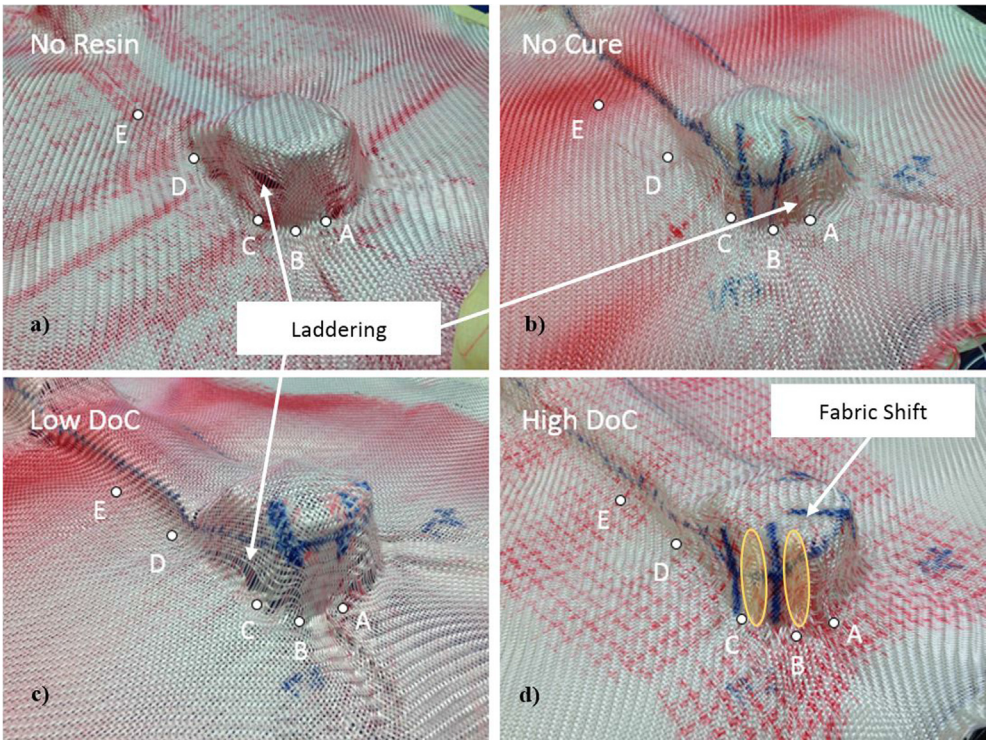

Fig. 12. Forming images from case study 1 (a) unstiffened fabric (b) stiffened with uncured resin (c) low degree of cure (d) high degree of cure. (For interpretation of the references to colour in this figure legend, the reader is referred to the web version of this article.)

4.3.2. Line patching case study 2

In order to address the problem of laddering, a very thin sheet of release film was placed between the mould and the fabric on both sides which significantly reduced friction. The low thickness of the film material ensured that it had negligible resistance and consequently no effect on the formability other than to reduce friction. The unstiffened case and the low degree of cure case from Case Study 1 were then repeated with this amendment to the setup. The results of this case study are shown in Fig. 14 and Fig. 15.

It is apparent that this setup produces a significantly higher quality component that previous attempts. Both in the stiffened and unstiffened manufacturing trials wrinkles were largely suppressed. The dry fabric has minor wrinkles in three of the four corners whereas the low degree of cure sample has minor wrinkles in just two. Generally these wrinkles are occurring just outside the perimeter of the actual component with just one notable case for the unstiffened fabric where these wrinkles make major inroads into the component itself. However, a near defect free component was achieved only for the stabilized materials. In dry fabric laddering occurs on the top region of the shape, whereas this has been avoided entirely in the stiffened sample. Therefore, on the basis of this experiment it has been possible to achieve a higher quality component through the placement of resin patches.

5. Conclusions

The results presented in this study give strong evidence that local

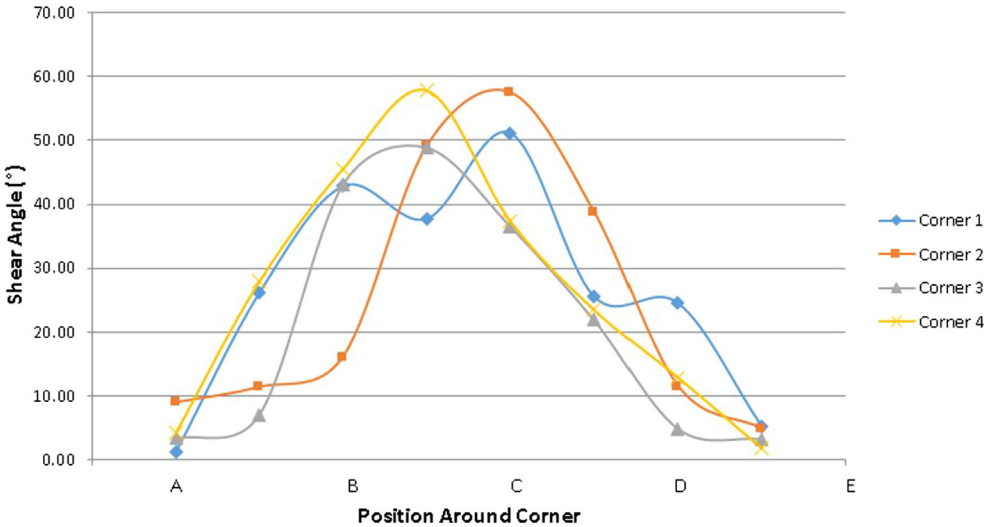

Fig. 13. Shear map of the line patch injected fabrics (low DoC). (For interpretation of the references to colour in this figure legend, the reader is referred to the web version of this article.)

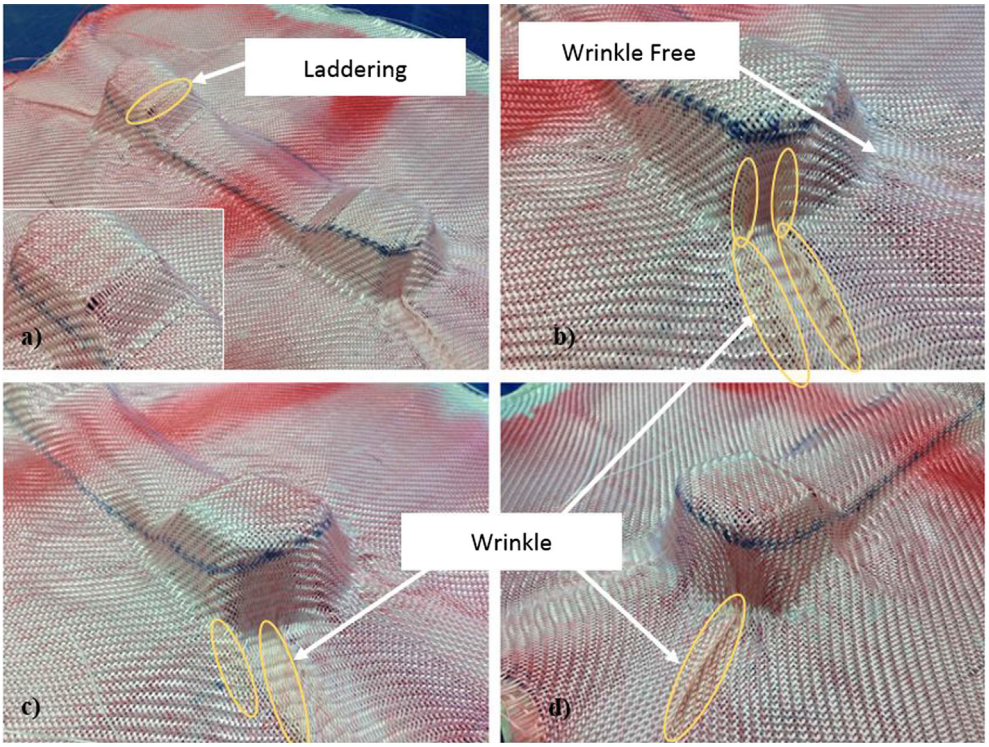

Fig. 14. Forming images from case study 2 for unstiffened fabric (a) full View (b) corner 1 (c) corner 3 (d) corner 4 (rotating sample clockwise). (For interpretation of the references to colour in this figure legend, the reader is referred to the web version of this article.)

stabilisation of fabric by means of reactive resin injection is a promising method that can enrich the palette of techniques available for defect mitigation in forming. Compared to other methods it has several advantages, including simplicity of implementation – no additional fabric constraints are required, flexibility and good potential for automation, and non-interference with reinforcement geometry – the yarn architecture is not affected by resin deposition compared with through-thickness reinforcements. It was shown that fine tuning of preform properties can help to achieve a near defect free component. On the other hand, the implementation of this approach bears additional

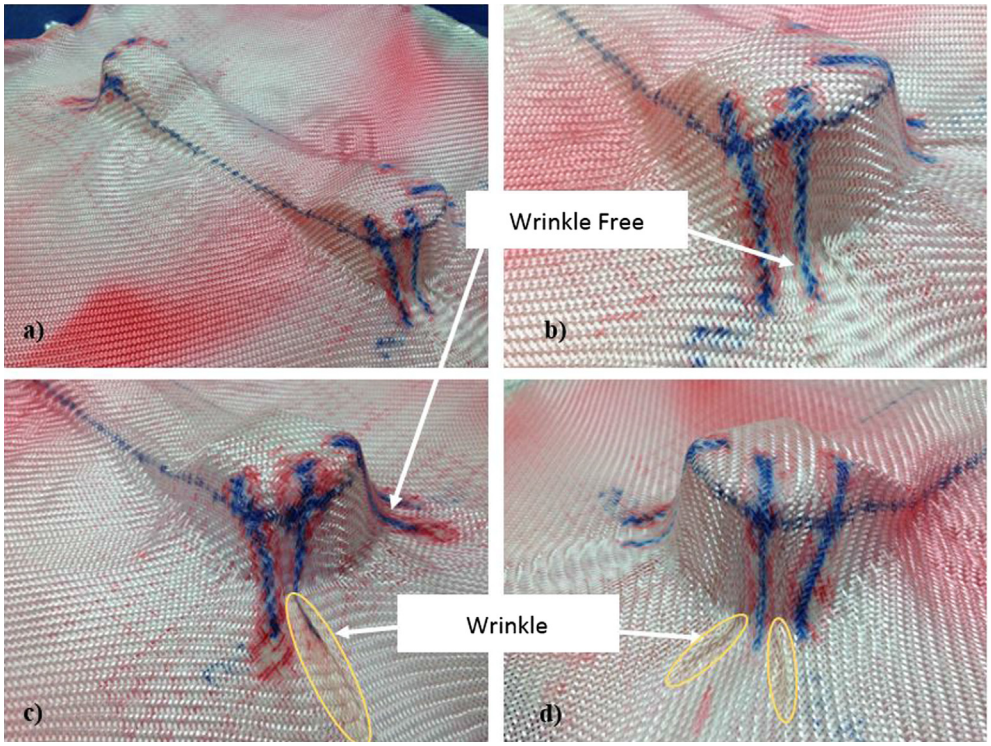

Fig. 15. forming images from case study 2 for low degree of cure (a) full view (b) corner 1 (c) corner 3 (d) corner 4 (rotating sample clockwise). (For interpretation of the references to colour in this figure legend, the reader is referred to the web version of this article.)

complexity. As shown in the paper, forming patterns are strongly influenced not only by the patch position and geometry but also by the balance of properties between patches and bulk fabric, though varying bending rigidity of the patches in the range of 0.01 N mm^2–100 N mm^2 did not reveal a clear impact on the forming pattern. Hence, sophisticated forming process modelling tools for mapping the resin deposition, fine tuning the viscosity of deposited resin, and extensive characterisation of resin and fabric are required.

The parameters influencing the forming shape a vast design space. The two-step optimisation used in this study, although pragmatic and simple, shows how the search for an acceptable solution can be organised. The idea that favourable position of patched regions can be dictated by the shear intensity overall agrees with conventional approaches to forming assessment, but it is clearly seen that it cannot be used alone. Defining the fine geometry of the patches requires higher fidelity simulation with direct observation of wrinkling. An essential hint in selecting patch orientation is that shearing must be impeded while the impact on bending minimised, which leads to an unusual off-fibre patch orientation.

It is important to emphasize that the simulations were used as a design tool only and direct comparison with experiments cannot be made at this stage. To have a full realistic analysis of wrinkle shape and severity all the material properties would need to match experimental reality. This raises a question about how the shearing and bending resistance of the patch could be measured - an interesting question for which no readily available techniques for such measurements currently exist. A plausible approach could be built around running numerical models and experiments concurrently (e.g., in a bias extension test) and using reverse property identification to match local deformation over the preform volume. Another limitation of the model, that prevents its direct validation in the considered cases, is that it does not take into account preform fibre slippage (laddering) – substantial defects that must be avoided in manufacturing practice.

The conclusions drawn in this paper are applicable to biaxial architectures with an initially orthogonal system of fibres, i.e., single plies of woven preforms. Whether a similar technique can be applicable to multi-layer forming is yet to be explored. Due to the additional constraints and mechanisms of consolidation in the multilayer scenario this possibly represents a different challenge. On the other hand, local patching may pave the way for an alternative approach in manufacturing where each of the plies in a laminate can be addressed separately. We can envisage a manufacturing process where multi-ply stack is assembled from plies patched and preformed in isolation and in advance. Such pre-conditioning can also be efficiently automated and address consolidation defects as well as forming ones.

Overall, the experimental trials, informed by modelling, prove the potential of the envisaged approach. The experimental work confirmed the importance of tuning patch geometry and properties, showed the advantage of local patching compared to powder binder stabilisation, and highlighted other essential factors where local stabilisation can play an important role – such as tool-preform friction. It was demonstrated that with careful patch parametrisation in the numerical solution, shear can be redistributed around critical regions and the quality of the manufacturing trials improved when compared to a reference non-assisted forming, even when the tool-preform friction is optimised.

Declaration of Competing Interest

The authors declared that there is no conflict of interest.

Acknowledgements

The work of Vermes, Thompson, Belnoue and Hallett has been supported by GKN Aerospace and the EPSRC Platform Grant [EP/P027350/1] SIMulation of new manufacturing PROcesses for Composite Structures (SIMPROCS).

The work of Turk and Ivanov has been supported by the EPSRC through the Future Composites Manufacturing Research Hub [EP/P006701/1].

Authors express gratitude to GKN Aerospace for productive discussion and for producing the Styrene Acrylate moulds for this project printed using Fused Deposition Modelling (FDM) technology at GKN Aerospace Filton.

All underlying data are provided in full within this paper.

Appendix A. Supplementary material

Supplementary data to this article can be found online at https://doi.org/10.1016/j.compositesa.2019.105643.

References

[1] Nezami NF, Gereke T, Cherif C. Active forming manipulation of composite reinforcement for the suppression of forming defects. Compos A 2017;99:94–101.
[2] Lee JS, Hong SJ, Yu WR, Kang TJ. The effect of blank holder force on the stamp forming behavior of non-crimp fabric with a chain stitch. Compos Sci Technol 2007;67(3–4):357–66.
[3] Allaoui S, Boisse P, Chatel S, Hamila N, Hivet G, Soulat D, et al. Experimental and numerical analyses of textile reinforcement forming of a tetrahedral shape. Compos A Appl Sci Manuf 2011;42(6):612–22.
[4] Zhu B, Yu TX, Zhang H, Tao XM. Experimental investigation of formability of commingled woven composite preform in stamping operation. Compos B 2011;42:289–95.
[5] Boisse P, Hamila N, Madeo A. Modelling the development of defects during composite reinforcements and prepreg forming. Philosop Trans Royal Soc A Math Phys Eng Sci 2016:374.
[6] Chen S, Harper LT, Endruweit A, Warrior NA. Formability optimisation of fabric preforms by controlling materialdraw-in through in-plane constraints. Compos A 2015;76:10–9.
[7] Breuer U, Neitzel M. Deep drawing of fabric-reinforced thermoplastics: wrinkle formation and their reduction. Polym Compos 1996;17:643–7.
[8] Molnar P, Ogale A, Lahr R, Mitchang P. Influence of drapability by using stitching technology to reduce fabric deformation and shear during thermoforming. Compos Sci Technol 2007;67(15–16):3386–93.
[9] Liu L, Zhang T, Wang P, Legrand X, Soulat D. Influence of the tufting yarns on formability of tufted 3-dimensional composite reinforcement. Compos A 2015;78:403–11.
[10] Dobrich O, Gereke T, Cherif C. Drape simulations: Textile material model for correct property reproduction to improve the preform development process of fiber-reinforced structures. Proceedings of the 12th International LS-Dyna conference. Deraborn; 2012.
[11] Hubner M, Diestel O, Sennewald C, Gereke T, Cherif C. Simulation if the drapability of textile semi-finished products with gradient-drapability characteristics by varying the fabric weave. Fibres Text East Eur 2012;20(2):88–93.
[12] Mouritz AP, Leong KH, Herszberg I. A review of the effect of stitching on the in-plane mechanical properties of fibre-reinforced polymer composites. Compos Part A Appl Sci Manuf 1997;28(12):979–91.
[13] Vermes B, Thompson A, Belnoue JP-H, Hallett SR, Ivanov DS. Mitigation Against Forming Defects by Local Modification of Dry Preforms. ECCM18. 18th European Conference on Composite Materials; 2018.
[14] Vermes B. Hybrid manufacturing concept for complex non-structural aerospace components. MSc Dissertation, University of Bristol, 11th Sept 2017.
[15] Ivanov DS, White JAP, Hendry W, Mahadik Y, Minett V, Patel H, et al. Stabilizing textile preforms by means of liquid resin print: a feasibility study. Adv Manuf: Polym Compos Sci 2014;1:26–35.
[16] Ivanov DS, Le Cahain YM, Arafati S, Dattin A, Ivanov SG, Aniskevich A. Novel method for functionalising and patterning textile composites: liquid resin print. Comp A 2016;84:175–85.
[17] Gereke T, Dobrich O, Hubner M, Cheriff C. Experimental and computational composite textile reinforcement forming: a review. Compos A 2013;46:1–10.
[18] Boisse P, Colmars J, Hamila N, Steer Q. Bending and wrinkling of composite fiber preforms and prepregs. A review and new developments in the draping simulations. Compos Part B 2018;141:234–49.
[19] Aimene Y, Hagefe B, Sidoroff F, Vidal-Salle E, Boisse P, Dridi S. Hyperelastic approach for composite reinforcement forming simulations. Int J Mater Form 2008;1:811–4.
[20] Peng X, Guo Z, Du T, Yu W-R. A simple anisotropic hyperelastic constitutive model for textile fabrics with application to forming simulation. Compos B 2013;52:275–81.
[21] Dangora LM, Mitchell CJ, Sherwood JA. Predictive model for the detection of out-of-plane defects formed during textile-composite manufacture. Compos A Appl Sci Manuf 2015;78:102–12.
[22] Khan MA, Mabrouki T, Vidal-Sallé E, Boisse P. Numerical and experimental analyses of woven composite reinforcement forming using a hypoelastic behaviour. Application to the double dome benchmark. J Mater Process Technol 2010;210(2):378–88. https://doi.org/10.1016/j.jmatprotec.2009.09.027.
[23] Boisse P, Zouari B, Daniel J-L. Importance of in-plane shear rigidity in finite element

analyses of woven fabric composite preforming. Compos A Appl Sci Manuf 2006;37:2201–12.
[24] Lebrun G, Bureau MN, Denault J. Evaluation of bias-extension and picture-frame test methods for the measurement of intraply shear properties of PP/glass commingled fabrics. Compos Struct 2003;61:341–52.
[25] Harrison Philip. Modelling the forming mechanics of engineering fabricsusing a mutually constrained pantographic beam and membrane mesh. Compos A 2016;81:145–57.
[26] Xiong Hu, Maldonado Eduardo Guzman. Nahiène Hamila, Philippe Boisse. A prismatic solid-shellfinite element based on a DKT approach withefficient calculation of through the thickness deformation. Finite Elem Anal Des 2018;151:18–33.
[27] Denis Y, Guzman-Maldonado E, Hamila N, Colmars J, Morestin F. A dissipative constitutive model for woven composite fabric under large strain. Compos A 2018;105:165–79.
[28] Skordos AA, Monroy Aceves C, Sutcliffe MPF. A simplified rate dependent model of forming and wrinkling of pre-impregnated woven composites. Comp A 2007;38(5):1318–30.
[29] Thompson A., Belnoue J.P-H., Hallett S.R. Numerical modelling of defect generation during preforming of multiple layers of 3D woven fabrics, Proceedings of ECCM17 conference, Munich, Germany, 26–30th 2016.
[30] Thompson A. Multi-Scale Modelling of Textile Composite Manufacture PhD Thesis University of Bristol; 2017.
[31] Haanappel SP, ten Thije R, Akkerman R. Forming Predictions of UD Reinforced Thermoplastic Laminates, ECCM14 Conference. Hungary: Budapest; 2010.
[32] Lightfoot JS, Wisnom MR, Potter K. A New Mechanism for the Formation of Ply Wrinkles Due to Shear Between Plies. Compos. Part A 2013;49:139–47.
[33] Allaoui S, Cellard C, Hivet G. Effect of inter-ply sliding on the quality of multilayer interlock dry fabric preforms. Compos A 2015;68:336–45.
[34] Wang P, Hamila N, Boisse P. Thermoforming simulation of multilayer composites with continuous fibres and thermoplastic matrix. Compos B 2013;52:127–36.
[35] Belnoue JP-H, Nixon-Pearson OJ, Thompson AJ, Ivanov DS, Potter KD, Hallett SR. Consolidation-driven defect generation in thick composite parts. J Manuf Sci Eng 2018;140(7). https://doi.org/10.1115/1.4039555.
[36] Cao J, Akkerman R, Boisse P, Chen J, Cheng HS, de Graaf EF, Gorczyca JL, Harrison P, Hivet G, Launay J, Lee W, Liu L, Lomov SV, Long A, de Luycker E, Morestin F, Padvoiskis J, Peng XQ, Sherwood J, Stoilova Tz, Tao XM, Verpoest I, Willems A, Wiggers J, Yu TX, Zhu B. Characterization of mechanical behavior of woven fabrics: Experimental methods and benchmark results. Compos A Appl Sci Manuf 2008;39(6):1037–53. https://doi.org/10.1016/j.compositesa:2008.02.016.
[37] Lin Hua, Clifford Mike J, Long Andrew C, Sherburn Martin. Finite element modelling of fabric shear. Modelling Simul. Mater. Sci. Eng. 2009;17(1):015008. https://doi.org/10.1088/0965-0393/17/1/015008.
[38] Matveev Mikhail Y, Endruweit Andreas, De Focatiis Davide SA, Long Andrew C, Warrior Nicholas A. A novel criterion for the prediction of meso-scale defects in textile preforming. Compos Struct 2019;226:111263.